AD-A074 375 TECHNION - ISRAEL INST OF TECH HAIFA MATERIAL MECHAN--ETC F/G 20/11
DYNAMIC RESPONSE OF A SLAB OF ELASTIC-VISCOPLASTIC MATERIAL THA--ETC(U)
AUG 79 J ABOUDI, S R BODNER F49620-79-C-0196

UNCLASSIFIED MML-67 AFOSR-TR-79-0964 NL

| OF |

ADA
074375

END
DATE
FILMED
10 -79
DDC

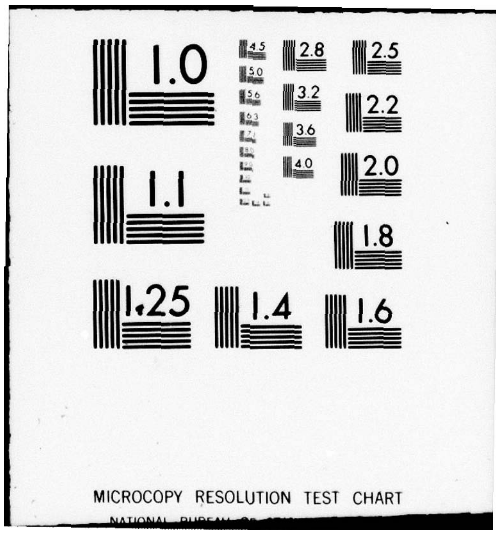
1.0
1.1
1.25
1.4
1.6
1.8
2.0
2.2
2.5
2.8
3.2
3.6
4.0
4.5
5.0
5.6
6.3
MICROCOPY RESOLUTION TEST CHART

Contract No. F49620-79-C-0196

AFOSR-TR- 79-0964

LEVEL II

Catalogue No.: IS ISSN 0072-9310

DYNAMIC RESPONSE OF A SLAB OF ELASTIC-VISCOPLASTIC MATERIAL THAT EXHIBITS INDUCED PLASTIC ANISOTROPY

by

J. ABOUDI and S. R. BODNER

MML Report No. 67

MATERIAL MECHANICS LABORATORY
FACULTY OF MECHANICAL ENGINEERING
TECHNION—ISRAEL INSTITUTE OF TECHNOLOGY
HAIFA, ISRAEL

August 1979

Scientific Report No. 1

prepared for
AIR FORCE OFFICE OF SCIENTIFIC RESEARCH/NA
Building 410, Bolling AFB, D.C. 20332
and
EUROPEAN OFFICE OF AEROSPACE RESEARCH AND DEVELOPMENT
London, England

Approved for public release; distribution unlimited.

(14) MML-67, SCIENTIFIC-1

REPORT DOCUMENTATION PAGE

READ INSTRUCTIONS BEFORE COMPLETING FORM

1. Report Number	2. Govt Accession No.	3. Recipient's Catalog Number
(6) 4. Title (and Subtitle) DYNAMIC RESPONSE OF A SLAB OF ELASTIC-VISCOPLASTIC MATERIAL THAT EXHIBITS INDUCED PLASTIC ANISOTROPY		5. Type of Report & Period Covered Scientific (Interim) (1979) 6. Performing Org. Report Number MML Report No. 67
7. Author(s) (10) J. Aboudi ~~and~~ S.R. Bodner		8. Contract or Grant Number (15) F49620-79-C-0196
9. Performing Organization Name and Address Material Mechanics Laboratory Faculty of Mechanical Engineering Technion - Israel Institute of Technology Haifa 32000, Israel		10. Program Element, Project, Task Area & Work Unit Numbers (12) 41p.
11. Controlling Office Name and Address Air Force Office of Scientific Research (NA) Bolling AFB, Bldg. 410 Washington, D.C. 20332		12. Report Date (11) Augu~~st~~ 1979 13. Number of Pages 37
14. Monitoring Agency Name and Address EOARD (Box 14) FPO NY 09510 (16) 2307 (17) B1		15. (18) AFOSR (19) TR-79-0964

16. & 17. Distribution Statement

Approved for public release; distribution unlimited.

18. Supplementary Notes

19. Key Words

Constitutive Equations	Work Hardening
Viscoplasticity	Indentation
Anisotropy	Dynamic Loading

20. Abstract

Various two-dimensional problems of the dynamic loading of a slab are solved for a material characterization that is elastic-viscoplastic and exhibits anisotropic work-hardening. The governing constitutive equations are based on a unified formulation which requires neither a yield criterion nor loading or unloading conditions. They include multi-dimensional anisotropic effects induced by the plastic deformation history. The theory also considers plastic compressibility which depends on the extent of anisotropy. A numerical procedure for solving equations is developed which incorporates the history dependent anisotropic hardening effects. Cases considered are the dynamic penetration of a slab by a rigid cylindrical indenter, and a distributed force rapidly applied over part of the slab surface. Both conditions of fixed and free rear surfaces of the slab are examined. A uniaxial problem is also considered in which different bases for the anisotropic hardening law are examined.

FORM 1473

401 910

DYNAMIC RESPONSE OF A SLAB OF ELASTIC-VISCOPLASTIC MATERIAL THAT EXHIBITS INDUCED PLASTIC ANISOTROPY

by

J. Aboudi[1] and S.R. Bodner[2]

ABSTRACT

Various two-dimensional problems of the dynamic loading of a slab are solved for a material characterization that is elastic-viscoplastic and exhibits anisotropic work-hardening. The governing constitutive equations are based on a unified formulation which requires neither a yield criterion nor loading or unloading conditions. They include multi-dimensional anisotropic effects induced by the plastic deformation history. The theory also considers plastic compressibility which depends on the extent of anisotropy. A numerical procedure for solving the equations is developed which incorporates the history dependent anisotropic hardening effects. Cases considered are the dynamic penetration of a slab by a rigid cylindrical indenter, and a distributed force rapidly applied over part of the slab surface. Both conditions of fixed and free rear surfaces of the slab are examined. A uniaxial problem is also considered in which different bases for the anisotropic hardening law are examined.

---

1 Associate Professor, Department of Solid Mechanics, Materials and Structures, Tel Aviv University, Ramat Aviv.

2 Professor, Faculty of Mechanical Engineering, Technion, Haifa.

INTRODUCTION

A unified theory for elastic-viscoplastic isotropic work-hardening materials which has the property that it requires neither a yield criterion nor loading or unloading conditions has been proposed by Bodner and Partom [1]. In this formulation, both elastic and inelastic deformations are present at all stages of loading and unloading. This theory was implemented in several two-dimensional dynamic indentation problems by Aboudi [2] and extensive investigations were made concerning the effect of the viscoplastic mechanism.

The isotropic theory ignores, however, the existence of the Bauschinger effect which expresses the observation that material hardening in a given direction of stressing causes a reduction of hardening in the opposite direction. In a multi-axial situation, the material develops changes in resistance to plastic flow (hardening) which vary in orientation as well as with the sign of the stresses (or the inelastic deformation rates). The resistance to plastic flow is therefore anisotropic and depends upon the complete loading history.

In order to incorporate these effects, the theory was generalized by Stouffer and Bodner [3] to include anisotropic work-hardening. This is achieved by the development of suitable evolutionary equations for the inelastic state variables which represent the varying resistance of the material to plastic flow in direction and in orientation. According to the equations of [3], part of the rate of change of a state variable is isotropic and the remaining part depends upon the relative sign and orientation of the current rate of deformation vector. As a consequence of the induced anisotropic hardening, plastic flow of an initially isotropic material becomes anisotropic and compressible.

In the present paper, the theory of anisotropic hardening is implemented on two-dimensional dynamic problems to investigate the effect of non-isotropic work-hardening. A numerical procedure is proposed which generalizes the previous one described in [2] by including the dependence of hardening on the complete history of deformation. The method is applied to a class of dynamic indentation problems in which the contact region between the indenter (assumed to be rigid) and the elastic-viscoplastic solid is not known in advance but must be determined as part of the solution. The proposed procedure is also applied to a thick slab which is excited by an extended time-dependent normal loading on its surface, while the other surface is either rigidly clamped or traction-free. The effects of the induced anisotropic hardening and the consequent anisotropic plastic flow are shown in each case, and comparisons are made with corresponding results obtained from the isotropic theory.

Finally, the method is illustrated in a uniaxial problem of an elastic-viscoplastic rod which is impacted by a time-dependent loading. Here we also investigate the effect of different reference bases for the non-isotropic hardening law, i.e. the physical quantities that could govern hardening. These could be either the current plastic deformation rate (as in [3]), or the current direct stress. Compressibility effects associated with each case are also calculated, and the results are compared with each other and with those of the isotropic theory.

BASIC THEORY

The constitutive equations for elastic-viscoplastic materials with isotropic work-hardening proposed by Bodner and Partom [1] have the basic property that no yield criterion nor loading or unloading conditions are required. In the framework of these equations, both elastic and inelastic deformations are present at all stages of loading and unloading although one type of deformation might be negligibly small in some loading regimes. For infinitisimal strains (considered in the present case), the constitutive equations of the material can be described by separating the total strain rate components into elastic (reversible) and plastic (non-reversible) strain rates as follows

$$\dot{\varepsilon}_{ij} = \dot{\varepsilon}_{ij}^{(e)} + \dot{\varepsilon}_{ij}^{(p)} \qquad i,j = 1,2,3 \qquad (1)$$

where the strains are given by $\varepsilon_{ij} = (u_{i,j} + u_{j,i})/2$ with u_i being the components of the displacement vector and the dots representing time derivatives.

The elastic strain rates $\dot{\varepsilon}_{ij}^{(e)}$ are related to the stress rates $\dot{\sigma}_{ij}$ according to the usual Hooke's Law (assuming elastic isotropy),

$$\dot{\varepsilon}_{ij}^{(e)} = \dot{\sigma}_{ij}/2\mu - \lambda\dot{\sigma}_{kk}\delta_{ij}/[2\mu(3\lambda+2\mu)] \qquad (2)$$

where λ, μ are the Lamé constants of the material and δ_{ij} is the Kronecker delta.

In the most general anisotropic plastic flow rule, the plastic strain rates are related to the stresses according to [3],

$$\dot{\varepsilon}_{ij}^{(p)} = \hat{\Lambda}_{ijk\ell} s_{k\ell} \qquad i,j,k,\ell = 1,2,3 \tag{3}$$

where $\hat{\Lambda}_{ijk\ell}$ is a fourth order tensor valued function and s_{ij} denotes the deviators of the stress tensor, i.e., $s_{ij} = \sigma_{ij} - \sigma_{kk}\delta_{ij}/3$. The symmetry properties of $\dot{\varepsilon}_{ij}^{(p)}$ and s_{ij} imply that

$$\hat{\Lambda}_{ijk\ell} = \hat{\Lambda}_{jik\ell} = \hat{\Lambda}_{ij\ell k} \tag{4}$$

Following Stouffer and Bodner [3], let us rewrite (3) in a 6-dimensional vector space in the following form (the summation convention does not apply to this paper on Greek letters):

$$\hat{D}_{\alpha} = \sum_{\beta=1}^{6} \hat{\Lambda}_{\alpha\beta}\hat{T}_{\beta} \qquad \alpha,\beta=1,\ldots,6 \tag{5}$$

where

$$\begin{aligned}
\hat{D}_1 &= \dot{\varepsilon}_{11}^{(p)} , & \hat{T}_1 &= s_{11} ,\\
\hat{D}_2 &= \dot{\varepsilon}_{22}^{(p)} , & \hat{T}_2 &= s_{22} ,\\
D_3 &= \dot{\varepsilon}_{33}^{(p)} , & \hat{T}_3 &= s_{33} ,\\
\hat{D}_4 &= \sqrt{2}\ \dot{\varepsilon}_{12}^{(p)} , & \hat{T}_4 &= \sqrt{2}\ s_{12} ,\\
\hat{D}_5 &= \sqrt{2}\ \dot{\varepsilon}_{23}^{(p)} , & \hat{T}_5 &= \sqrt{2}\ s_{23} ,\\
\hat{D}_6 &= \sqrt{2}\ \dot{\varepsilon}_{13}^{(p)} , & \hat{T}_6 &= \sqrt{2}\ s_{13} ,
\end{aligned} \tag{6}$$

and $\hat{\Lambda}_{\alpha\beta}$ is a 6 x 6 tensor.

By a proper orthogonal transformation we can reduce (5) to the form

$$D_\alpha = \sum_{\beta=1}^{6} \Lambda_{\alpha\beta} T_\beta \tag{7}$$

where $\Lambda_{\alpha\beta}$ is a 6 x 6 <u>diagonal</u> tensor.
The rate of plastic deformation D_α and the stress deviators T_α form, respectively, two vectors $\underset{\sim}{D}$ and $\underset{\sim}{T}$ each of six components in the 6-dimensional space, whose bases are $\underset{\sim}{e}_\alpha$, in which the tensor $\Lambda_{\alpha\beta}$ is diagonal (see [3] for more details). Corresponding to the Prandtl-Reuss equations for isotropic plastic flow, (7) implies that the plastic deformation rate components D_α are parallel to the corresponding deviator T_α. On the other hand, the anisotropic plastic flow rule (7) does not lead to incompressible plastic deformation since, in general, $\Lambda_{11} \neq \Lambda_{22} \neq \Lambda_{33}$ so that $D_1 + D_2 + D_3 \neq 0$. For the case of isotropic plastic flow, however, $\Lambda_1 = \Lambda_2 = \Lambda_3 \equiv \Lambda$ which implies that $D_1 + D_2 + D_3 = 0$. In this special case, plastic deformation is necessarily isochoric for every choice of Λ.

A unified elastic-viscoplastic non-isotropic work-hardening theory is achieved by assuming that each non-zero component $\Lambda_{\alpha\beta}$ (i.e. the diagonal terms $\Lambda_{\alpha\alpha}$) can be expressed in terms of a single valued scalar function of the second invariant of the deviatoric stress tensor $J_2 (J_2 = s_{ij}s_{ij}/2)$, the temperature T and the state variables $Z_{\alpha\beta}$. The terms $Z_{\alpha\beta} = 0$ for $\alpha \neq \beta$ so that each non-zero component $Z_{\alpha\beta}$ corresponds directly to a non-zero component $\Lambda_{\alpha\beta}$, i.e.

$$\Lambda_{\alpha\alpha} = F(J_2, T, Z_{\alpha\alpha}) \tag{8}$$

The quantities $Z_{\alpha\beta}$ are referred to as the hardness variables of the material which express its resistance to plastic flow. They are used to describe the state of the material microstructure at any time t and thereby depend upon the complete history of the deformation up to the current time.

Due to the Bauschinger effect, the response of the material in tension and compression or shear to the left and right are different as a result of which the material develops anisotropic plastic flow. Accordingly, we define

$$Z_{\alpha\alpha}(t) = \begin{cases} Z^{+}_{\alpha\alpha}(t) & D_{\alpha}(t) > 0 \\ Z^{-}_{\alpha\alpha}(t) & D_{\alpha}(t) < 0 \end{cases} \tag{9}$$

where $Z^{+}_{\alpha\alpha}(t)$ and $Z^{-}_{\alpha\alpha}(t)$ are the hardness variables for positive and negative plastic deformation rates, respectively, (following [3]).

A specific form for the evolution laws for $Z_{\alpha\alpha}(t)$ is given in [3] in the form

$$\dot{Z}_{\alpha\alpha}(t) = \begin{cases} q\dot{z}(t) + (1-q)\dot{z}\, r_{\alpha}(t) & D_{\alpha}(t) > 0 \\ q\dot{z}(t) - (1-q)\dot{z}\, r_{\alpha}(t) & D_{\alpha}(t) < 0 \end{cases} \tag{10}$$

where z(t) is a single valued monotonically increasing function of the total plastic work $W_p(t)$ such that an increase in z(t) corresponds to an increase in the resistance of the material to plastic flow. This implies that the hardness of the material is taken to depend on the amount of plastic work which has been done on the material from a reference state. In (10), q is a material parameter describing the relative amount of hardening that is isotropic, and $r_\alpha(t)$ are taken, following [3], to be the "direction cosines" of the rate of deformation vector:

$$r_\alpha(t) = D_\alpha(t)/|\underset{\sim}{D}(t)| \tag{11}$$

with

$$|\underset{\sim}{D}|^2 = \underset{\sim}{D} \cdot \underset{\sim}{D}$$

The evolution equations (10) for the state variables which control the hardness of the material indicate that part of the rate of change is isotropic and the remaining part varies according to the sign and orientation of the current rate of deformation vector. When q = 1, the completely isotropic work-hardening situation is obtained in which all the $\Lambda_{\alpha\alpha}$ are equal and plastic deformation is incompressible. The case $q < 0$ is admissible, e.g. cyclic softening.

Integration of the evolution equations (10) yields

$$\underset{\sim}{Z}(t) = \overset{(o)}{\underset{\sim}{Z}} + \underset{\sim}{e}_\alpha \int_o^t q\dot{z}(\tau)d\tau +$$

$$\underset{\sim}{e}_\alpha \, \mathrm{sign}[D_\alpha(t)] \int_o^t (1-q)\dot{z}(\tau)r_\alpha(\tau)d\tau \tag{12}$$

where $\underset{\sim}{Z}(t) = \sum_{\alpha=1}^{6} Z_{\alpha\alpha}(t)\underset{\sim}{e}_\alpha$ is a 6-dimensional vector described by the base vectors $\underset{\sim}{e}_\alpha$, and $\overset{(o)}{\underset{\sim}{Z}}$ represents the initial hardness in each of the six coordinate directions. Equation (12) expresses the dependence of the hardness of the material on the deformation path. The second term in (12) represents the total isotropic hardening up to time t, whereas the total anisotropic hardening used to characterize the multi-axial Bauschinger effect is given by the last term. As a consequence of (12), the components of $\underset{\sim}{Z}$ at the current time t have different values which gives induced anisotropic plastic flow.

Representation of the anisotropic plastic flow can be completely determined by specifying $\Lambda_{\alpha\alpha}$ in (8) and $\dot{z}(t)$ in (10). Motivated by equations relating dislocation velocities and stresses, Bodner and Partom [1] proposed a relation which can be generalized here for isothermal anisotropic hardening in the form

$$\Lambda_{\alpha\alpha} = D_o \exp[-\frac{n+1}{2n}(Z^2_{\alpha\alpha}/3J_2)^n]/J_2{}^{1/2} \qquad (13)$$

where D_o is the limiting value in shear of the strain rate of the material for high stresses and n is a specific parameter. The function $\dot{z}(t)$ in (10) is chosen to have the form

$$\dot{z}(t) = m(z_1 - z_o)\exp[-mW_p(t)/z_o]\dot{W}_p(t) \qquad (14)$$

so that

$$z(t) = z_1 - (z_1 - z_o)\exp[-mW_p(t)/z_o] \qquad (15)$$

The rate of the plastic work is given by

$$\dot{W}_p = \sum_{\alpha=1}^{6} T_\alpha D_\alpha + \text{trace } (\sigma_{ij})(D_1+D_2+D_3)/3 \qquad (16)$$

and it should be noticed that the trace is an invariant quantity. In (14), z_o, z_1 and m are appropriate parameters characterizing the material.

It is seen from (15) that an increase in the plastic work W_p corresponds to an increase in z which implies an increase of the resistance of the material to plastic flow. Equation (7) and (13) would lead directly to isotropic plastic flow as in [1] by choosing $Z_{\alpha\alpha} = z$ for all α. For the general case of anisotropic plastic flow, $Z_{\alpha\alpha}(t)$ in (13) is obtained by substituting $\dot{z}(t)$ of (15) into (12). The anisotropic plastic representation (12), (13) and (15) requires the use of five material constants q, n, m, z_o, z_1 which must be determined experimentally (D_o is actually a scale factor).

Returning to equation (7), it is necessary to know the orthogonal transformation which diagonalizes the material tensor $\hat{\Lambda}_{\alpha\beta}$ of (5). In the diagonal form $\Lambda_{\alpha\beta}$ and $Z_{\alpha\beta}$ are given with respect to the basis vectors $\underset{\sim}{e}_\alpha$. If the material is initially isotropic $Z_{\alpha\alpha}(o) = \overset{(o)}{Z}_{\alpha\alpha} = z_o$ for all α, and $Z_{\alpha\beta} = \Lambda_{\alpha\beta} = 0$ for $\alpha \neq \beta$ so that $\Lambda_{\alpha\beta}$ is in diagonal form. Consequently, any set of independent vectors $\underset{\sim}{e}_\alpha$ can be chosen as the basis vectors. As the deformation proceeds, the $Z_{\alpha\alpha}$ terms determined from (12) become different from each other and give rise to anisotropic plastic flow according to (13).

Formulation of the Problem

In this paper, we consider the dynamic response of a slab $-\infty<x_1<\infty$, $0\leq x_2\leq H$ under plane strain conditions. The slab is made of an elastic viscoplastic anisotropic work-hardening material whose constitutive equations were described in the previous section.

The slab is initially at rest at time $t<0$. The surface $x_2 = H$ is assumed to be kept either traction-free

$$\sigma_{12} = \sigma_{22} = 0, \quad -\infty < x_1 < \infty, \quad x_2 = H, \ t > 0 \tag{17}$$

or rigidly clamped

$$u_1 = u_2 = 0, \quad -\infty < x_1 < \infty, \quad x_2 = H, \ t > 0 \tag{18}$$

Two different situations for the slab will be considered in this paper.

(1) Dynamic indentation by a rigid punch:

In this case, the surface $x_2 = 0$ of the slab is pressed at $t = 0$ by a rigid indenter. As the indenter penetrates the slab, there is a region on the surface $x_2 = 0$ which at first has traction-free boundary conditions but later are displacement conditions. The boundary of the slab conforms to the geometry of the rigid body at the contact region which, in general, is initially unknown and must be determined from the solution. Consequently, the appropriate boundary conditions for a frictionless contact are

$$\left.\begin{array}{l}\sigma_{21} = 0 \\ \\ u_2 \;\; = f(x_1,t)\end{array}\right\} |x_1| \leq X(t), \quad x_2 = 0,\ t > 0 \qquad (19)$$

and

$$\left.\begin{array}{l}\sigma_{21} = 0 \\ \\ \sigma_{22} = 0\end{array}\right\} |x_1| > X(t), \quad x_2 = 0,\ t > 0 \qquad (20)$$

where $f(x_1,t)$ is the prescribed x_2 displacement imposed over the time-dependent region of contact. The function $X(t)$ describes the boundary of the moving region, which is a priori unknown, with $X(0) = 0$.

(2) Dynamic excitation by time-dependent normal tractions:

Here we assume that extended normal tractions are applied on the surface $x_2 = 0$ so that

$$\left.\begin{array}{l}\sigma_{21} = 0 \\ \\ \sigma_{22} = g(x_1,t)\end{array}\right\} -\infty < x_1 < \infty, \quad x_2 = 0,\quad t > 0 \qquad (21)$$

with $g\ (x_1,t)$ describing the form of the spatial and temporal excitation.

The stress-strain relations in the plane strain conditions for which $\varepsilon_{13} = \varepsilon_{23} = \varepsilon_{33} = 0$ are obtained from (2) and (1) in the form.

$$\sigma_{ij} = \lambda[\varepsilon_{11}+\varepsilon_{22}]\delta_{ij}+2\mu\varepsilon_{ij}-\lambda\varepsilon_{kk}^{(p)}\delta_{ij}-2\mu\varepsilon_{ij}^{(p)} \qquad (22)$$

The displacements $u_1(x_1,x_2,t)$ and $u_2(x_1,x_2,t)$ are governed by the dynamic equations of motion. These follow by substituting (22) into the equilibrium equations:

$$\rho \ddot{u}_i = \sigma_{ij,j} \tag{23}$$

in the absence of body forces, with ρ being the density of the material. Substituting (22) into (23) leads to the equations of motion:

$$\rho \ddot{u}_1 = (\lambda+2\mu)u_{1,11} + \mu u_{1,22} + (\lambda+\mu)u_{2,12} - \lambda\varepsilon^{(p)}_{kk,1}$$
$$-2\mu(\varepsilon^{(p)}_{11,1} + \varepsilon^{(p)}_{12,2})$$

$$\rho \ddot{u}_2 = (\lambda+2\mu)u_{2,22} + \mu u_{2,11} + (\lambda+\mu)u_{1,12} - \lambda\varepsilon^{(p)}_{kk,2}$$
$$-2\mu(\varepsilon^{(p)}_{12,1} + \varepsilon^{(p)}_{22,2}) \tag{24}$$

For isotropic hardening, plastic deformation is incompressible, i.e., $\varepsilon^{(p)}_{kk} = o$ and (22), (24) reduce to those given in [2]. In the following section, we present a numerical procedure which enables us to solve the above mentioned dynamic problems.

Numerical Treatment

The numerical treatment of the two-dimensional dynamic problem for the viscoplastic slab, which was formulated in the previous section, is based on a finite difference procedure. This is performed by introducing a net of mesh sizes Δx_1, Δx_2 in the x_1 and x_2 directions respectively together with a time increment Δt. The present numerical treatment is a generalization of the procedure given in [2] for isotropic plastic flow.

The procedure can be divided into three parts. In the first part, the displacement components at interior points within the slab are computed from the equations of motion (24). In the second part, the inelastic variables are computed throughout the slab. Finally, the third part consists of the computation of the displacements at the boundaries $x_2 = 0$ and $x_2 = H$.

Part 1: The displacement components $u_1(x_1,x_2,t)$, $u_2(x_1,x_2,t)$ at interior points within the slab are governed by the dynamic equations (24). These are solved by replacing all the derivatives by their corresponding central difference expressions obtaining an explicit three-level system of difference equations. Thus, it is possible to compute the displacements u_1, u_2, at time $t + \Delta t$ provided their values at the previous and current steps $t - \Delta t$ and t, respectively, as well as the values of plastic strains $\varepsilon_{ij}^{(p)}$ at time t, are known throughout the medium. The form of this difference system of equations is essentially similar to that given in [4] in a perfectly elastic solid, and the additional inelastic terms add no basic difficulty. This system is of a second order accuracy, i.e., the error by which the exact solution of the dynamic equations (24) does not satisfy the corresponding difference equations at a point is of second order in the increments.

Part 2: In order to compute the inelastic variables, we denote the plastic strains by $E_\alpha(x_1,x_2,t)$ such that $\dot{E}_\alpha = D_\alpha$ with D_α defined in (7). The plastic strain and the plastic work are governed by (7) and (16) respectively with $\Lambda_{\alpha\alpha}$ given in (13). For the plane strain problem, these equations provide a system of five equations in the unknown plastic strains and the plastic work in terms of the variables at time t at any point in the region. These equations can be integrated to yield the E_α and W_p at time $t + \Delta t$ at a point of the slab provided that $\Lambda_{\alpha\alpha}(x_1,x_2,t)$ is known at that point.

In order to compute $\Lambda_{\alpha\alpha}(x_1,x_2,t)$ at a point at time t, the hardness $Z^{\pm}_{\alpha\alpha}(x_1,x_2,t)$ must be determined [see eqn.(13)]. This is achieved by employing (10) which leads approximately to

$$Z^{\pm}_{\alpha\alpha}(x_1,x_2,t) \simeq Z^{\pm}_{\alpha\alpha}(x_1,x_2,t-\Delta t) + q\Delta z(x_1,x_2,t)$$

$$+ (1-q)\Delta z(x_1,x_2,t)r(x_1,x_2,t-\Delta t) \qquad (25)$$

where Δz is computed from

$$\Delta z(x_1,x_2,t) \simeq \dot{z}(x_1,x_2,t)\Delta t \tag{26}$$

The term $\dot{z}$ in (26) is approximated according to (14-15) by

$$\dot{z}(x_1,x_2,t) = m[z_1-z(x_1,x_2,t)]\dot{W}_p(x_1,x_2,t-\Delta t) \tag{27}$$

and $Z^{\pm}_{\alpha\alpha}(x_1,x_2,0) = z_o$ assuming that the material is initially isotropic.

Having computed $Z^{\pm}_{\alpha\alpha}(x_1,x_2,t)$ from (25), (9) can be used to determine $Z_{\alpha\alpha}(x_1,x_2,t)$. This is then employed in (13) to obtain $\Lambda_{\alpha\alpha}(x_1,x_2t)$ so that (7) and (16) can serve to provide the values of $D_\alpha(x_1,x_2,t)$ and $\dot{W}_p(x_1,x_2,t)$ respectively.

Equations (7) and (16) can be integrated to give the plastic strains and plastic work at time $t+\Delta t$ by using the improved Euler-Cauchy method. According to this method E_α and W_p at time $t+\Delta t$ are tentatively predicted from

$$\left.\begin{aligned} \overset{*}{E}_\alpha(x_1,x_2,t+\Delta t) &= E_\alpha(x_1,x_2,t) + \Delta t D_\alpha(x_1,x_2,t) \\ \overset{*}{W}_p(x_1,x_2,t+\Delta t) &= W_p(x_1,x_2,t) + \Delta t\dot{W}_p(x_1,x_2,t) \end{aligned}\right\} \tag{28}$$

$$\alpha = 1, \ldots, 4$$

These values are corrected according to

$$E_\alpha(x_1,x_2,t+\Delta t) = E_\alpha(x_1,x_2,t)$$

$$+ \Delta t[D_\alpha(x_1,x_2,t) + \overset{*}{D}_\alpha(x_1,x_2,t+\Delta t)]/2$$

$$W_p(x_1,x_2,t+\Delta t) = W_p(x_1,x_2,t)$$

$$+[\dot{W}_p(x_1,x_2,t) + \overset{*}{\dot{W}}_p(x_1,x_2,t+\Delta t)]/2 \qquad (29)$$

and the stars over D_α and $\dot{W}_p$ indicate that these are evaluated using $\overset{*}{E}_\alpha(x_1,x_2,t+\Delta t)$ and $\overset{*}{W}_p(x_1,x_2,t+\Delta t)$. On the other hand, the evaluation of $\overset{*}{D}_\alpha$ and $\overset{*}{\dot{W}}_p$ requires the determination of $\overset{*}{\Lambda}_{\alpha\alpha}(x_1,x_2,t+\Delta t)$ and these can be computed after obtaining $Z^{\pm}_{\alpha\alpha}(x_1,x_2,t+\Delta t)$. This is performed in the same manner as in the computation of $Z^{\pm}_{\alpha\alpha}(x_1,x_2,t)$ according to (25), but using instead the starred quantities, i.e.,

$$Z^{\pm}_{\alpha\alpha}(x_1,x_2,t+\Delta t) \simeq Z^{\pm}_{\alpha\alpha}(x_1,x_2,t) + q\Delta\overset{*}{z}(x_1,x_2,t+\Delta t)$$

$$+ (1-q)\Delta\overset{*}{z}(x_1,x_2,t+\Delta t)r(x_1,x_2,t) \qquad (30)$$

Consequently, it is possible to compute the plastic strains and plastic work at any point within the region at the time $t+\Delta t$ when all the field variables are known at time $t-\Delta t$ and t.

Part 3: The boundary displacements at $x_2=0$ are determined according to the relevant boundary conditions [(19-20) for the indentation problem or (21) for the applied tractions]. For the dynamic indentation of the slab by a rigid body, the boundary conditions (19-20) at $x_2=0$ are imposed as in [2], taking into account the fact that the region of contact between the slab and the indenter is, in general, unknown in advance but must be determined as part of the solution. This was achieved by an iterative procedure which is continued until all the requirements of the indentation problem are satisfied simultaneously (see [2] for more details).

When time-dependent normal tractions are applied on the surface $x_2=0$, the boundary conditions are given by (21). These are imposed by approximating the derivatives in the x_1 direction by central difference expressions and the derivatives in the x_2 direction by forward difference expressions. Consequently, a system of algebraic equations in the unknown displacements at the boundary $x_2=0$ is obtained at every time step as follows:

$$
\begin{aligned}
&u_1(i\Delta x_1,x_2,t) - u_1(i\Delta x_1,x_2+\eta\Delta x_2,t)\\
&-\eta\{\varepsilon[u_2((i+1)\Delta x_1,x_2,t) - u_2((i-1)\Delta x_1,x_2,t)]\\
&-2\Delta x_2 E_4(x_1,x_2,t)\} = 0
\end{aligned}
$$

$$
\begin{aligned}
&u_2(i\Delta x_1,x_2,t) - u_2(i\Delta x_1,x_2+\eta\Delta x_2,t)\\
&-\eta\{\varepsilon\delta[u_1((i+1)\Delta x_1,x_2,t) - u_1((i-1)\Delta x_1,x_2,t)]\\
&-\Delta x_2[2\delta_1 E_2(x_1,x_2,t) + \delta(E_1(x_1,x_2,t) + E_2(x_1,x_2,t)\\
&+E_3(x_1,x_2,t)) + g(x_1,t)]\} = 0 \qquad (31)
\end{aligned}
$$

where

$$\varepsilon = \Delta x_2/(2\Delta x_1)\ ,\ \delta = \lambda/(\lambda+2\mu)\ ,\ \delta_1 = \mu/(\lambda+2\mu)\ ,$$

$$x_2 = o\ ,\ \eta = 1.$$

Since the loading under consideration is symmetrical about the x_2 axis, the points $x_1<0$ need not be considered, i.e., $i=0,1,2,\ldots$.

The traction free conditions (17) at the surface $x_2=H$ also gives the system of equations (31) but with $x_2=H$, $\eta=-1$, $g(x_1,t)=0$. As in the perfectly elastic problem [5], it is convenient and efficient, both from the rate of convergence and programming viewpoints, to solve the above system of equations by the Gauss-Seidel iterative procedure. Details of the proof of the convergence of the process are given in [5].

Applications

The proposed method has been applied to the problems of the dynamic indentation of a viscoplastic slab by a long rigid circular cylinder, and to that of a slab subjected to an extended normal load rapidly applied on the slab surface. Calculations were based on titanium as the slab material for which the elastic and plastic constants are given in [1]: $\lambda = 0.9366 \times 10^5$ N/mm^2, $\mu = 0.44 \times 10^5$ N/mm^2, $\rho = 4.87$ gm/cm^3, $z_o = 1150$ N/mm^2, $z_1 = 1400$ N/mm^2, $D_o = 10^4$ sec^{-1}, $n = 1$ and $m = 100$. The material parameter that prescribes the relative amount of isotropic hardening, q, was found in [6] to be $q = 0.05$ for titanium. This was obtained under uniaxial cyclic stressing conditions using the current direct stress as the reference for the relative hardening effects. The value $q = 0.05$ was used in these calculations although it is not exactly representative since the hardening "cosine law" in the present formulation is based on the current plastic deformation rate (11). Further studies on this subject were made in relation to the uniaxial stress problem discussed later in the paper.

The slab thickness was taken to be $H = c_o D_o^{-1}/5$ which means that a compressional elastic wave whose speed in the material is $c_o = [(\lambda+2\mu)/\rho]^{1/2}$ will propagate the distance 5H during the time interval D_o^{-1}. Results presented in this paper were obtained, as in [2], with the spatial increments $\Delta x_1/H = \Delta x_2/H = 0.1$ and the time step $c_o \Delta t/H = 0.05$.

(1) The dynamic indentation by a rigid long circular cylinder:

For a long rigid cylinder indenting the slab, the function $f(x_1,t)$ in (19) has the form

$$f(x_1,t) = p(t) - R + (R^2-x_1^2)^{1/2} \tag{32}$$

In this equation, $p(t)$ is the penetration distance of the indenter along the x_2-axis, i.e., $p(t) = u_2(0,0,t)$, and R is the radius of the cylinder. This is assumed to be much larger than the contact area so that the boundary conditions (19-20) are applicable. When the cylinder is pressed into the slab at a constant speed V, $p(t) = Vt$.

In Fig. 1, plots of the normal and tangential stresses σ_{22}, σ_{11}, the vertical displacement u_2, and the plastic work W_p are given versus the distance x_1 along the surface $x_2=0$ of the slab when $c_o t/H=2.5$ and 5 with $V/c_o = 0.05$ and $R/H=5$. The other surface of the slab is kept rigidly clamped so that (18) holds. In the same Figure, the plastic work along the plane of symmetry $x_1=0$ within the slab is also shown. The stresses are normalized with respect to $\sigma_o = \lambda+2\mu$.

These results are compared with those corresponding to completely isotropic plastic deformations, i.e. q=1. This comparison indicates that the effect of the anisotropic hardening on the stress field and the shape of the deformed surface of the slab is not significant in this case.

The plots of the plastic work W_p give an indication of the amount of plastic deformation at various points of the slab at a given time. The anisotropic hardening case is seen to lead to lower values of W_p compared with the isotropic one. This does not seem to appreciably influence the surface stress field nor the contact area or the force required to press the cylinder into the slab in this example.

It is interesting to compare the amount of plastic volume change $E(x_1,x_2,t) = \sum_{\alpha=1}^{3} E_\alpha(x_1,x_2,t)$ which is obtained in the case of anisotropic plastic flow. (When the flow is isotropic the plastic deformation becomes isochoric at all times so that $E(x_1,x_2,t) \equiv 0$). Table I presents $E(0,0,t)$ at several times after the initiation of the identation process. The Table clearly shows a monotonic increase with indentation of the volume change due to plastic deformation at the given point.

The present indentation problem was also examined for the case when the surface $x_2=H$ of the slab is kept traction-free so that (17) is applicable. Here too, the results for the stress field show similar correspondence between the anisotropic and isotropic hardening. Extensive studies of the response to dynamic indentation of a slab made of an elastic-viscoplastic isotropic work-hardening material can be found in [2].

(2) Applied time-dependent loading:

The viscoplastic slab is subjected to an extended normal time-dependent traction (21) at $x_2=0$ of the form

$$g(x_1,t) = \begin{cases} g_o \sin[\pi t/2t_m)] & t<t_m \\ & & ,|x_1| \le H \\ g_o & t>t_m \end{cases} \qquad (33)$$

and g $(x_1,t) = 0$ for $|x_1|>H$. In Fig. 2, the resulting stresses and plastic work are shown at $x_2=H/2$ versus x_1 when $c_o t/H = 2.5$ and 5 with $g_o/\sigma_o = 0.1$ and $c_o t_m/H = 2.5$ in (33). In this Figure we present also the plastic work along the plane of symmetry $x_1=0$ within the slab at the same times. These results are compared with those corresponding to the isotropic hardening case (q=1). In both cases, the other surface of the slab $x_2=H$ is assumed to be rigidly clamped (18). The comparison shows that when $c_o t/H = 2.5$, the resulting stress fields are still similar. When $c_o t/H = 5$, however, considerable differences occur in the stress fields between the two cases which exhibits the effect of anisotropic hardening.

In Fig. 3, we present the results for the same two cases as Fig. 2 but the surface $x_2=H$ of the slab is kept traction-free (17). Here the effect of the anisotropic hardening is less pronounced. The different results obtained in Figs. 2 and 3 are attributed to the clamped and free boundary conditions which affect the reflected stress waves differently.

Finally, Table II gives the amount of plastic volume change at the point $x_1=x_2=0$ at several times, when the surface $x_2=H$ of the slab is either rigidly clamped or traction-free.

(3) Uniaxial deformation due to dynamic loading:

In order to obtain better understanding of the effect of anisotropic hardening, the simplest one-dimensional problem of uniaxial dynamic loading of a thin rod of length H in the x_2 direction was considered. The rod was assumed to be made of elastic-viscoplastic anisotropic work - hardening material (titanium). In this case the only non-zero stress component is the axial stress σ_{22} so that (2) reduces to

$$\dot{\varepsilon}_{22}^{(e)} = \dot{\sigma}_{22}/E \tag{34}$$

where $E = \mu(3\lambda+2\mu)/(\lambda+\mu)$ is the Young's modulus of the material.

The constitutive equation (22) then reduces to

$$\sigma_{22} = E\varepsilon_{22} - E\varepsilon_{22}^{(p)}$$

with $\varepsilon_{22} = \partial u_2/\partial x_2$, so that (24) take the form

$$\rho\ddot{u}_2 = E(u_{2,22} - \varepsilon_{22,2}^{(p)}) \tag{35}$$

It is assumed that $x_2=0$ is loaded in the form

$$\sigma_{22} = \begin{cases} g_1 \sin(2\pi t/t_m) & t \leq t_m \\ 0 & t > t_m \end{cases} \tag{36}$$

with g_1 being an amplitude factor, and the other end is kept stress-free, i.e.

$$\sigma_{22} = 0 \qquad\qquad x_2 = H \tag{37}$$

This one-dimensional dynamic problem forms a special case of the two-dimensional formulation and the method of solution.

By solving the problem for $g_1/\sigma_o = 0.05$ and $c_o t_m/H = 0.5$ in (36), we find that the axial stresses when $q = 0.05$ are the same as those for $q=1$, i.e., the effect of anisotropic hardening is negligible for all times. It turns out that the resulting stresses saturate in this case so that the effect of anisotropic hardening would therefore be relatively small, e.g. [7], in accordance with our observation. On the other hand, choosing $g_1/\sigma_o = 0.005$ and $c_o t_m/H = 0.5$ in (36), for which the amplitude of the applied stress is in the vicinity of the yield stress, the effect of anisotropic hardening becomes fairly pronounced, Fig.4.

All the results presented in this paper were based on the assumption of [3] that the anisotropic change in resistance to plastic flow is in the direction of the deformation rate, so that the "cosine law" (11) for the rate of plastic deformation is applicable. Another possibility is to use a "cosine law" for the current stress which means that $r_\alpha(t)$ in (11) would be replaced by

$$r_\alpha(t) = \sigma_{ij}/(3J_2)^{1/2} \tag{38}$$

with obvious relations between α and i, j (see eq.(6)). Note that $(3J_2)^{1/2}$ is the "effective stress". In a uniaxial problem,

(38) gives $r_2 = 1$ for $\sigma_{22} > 0$ and $r_2 = -1$ for $\sigma_{22} < 0$. As previously mentioned, the relative amount of isotropic hardening, q in (10), was determined for titanium in [6] using this rule.

It would be interesting, therefore, to compare the effects of anisotropic hardening using either (38) or (11). This comparison also appears in Fig. 4 which exhibits the axial stress and plastic work versus time at the observation point H/2 at the middle of the rod when it is loaded according to (36) with $g_1/\sigma_o = 0.005$ and $c_o t_m/H = 0.5$. It is seen that these two cosine laws do not lead to appreciable differences in this case. A consequence of this observation is that the value of q chosen to match a given uniaxial stress response should not be sensitive to the choice of either anisotropic hardening law. Fig. 4 shows, however, that the response is considerably different when hardening is assumed to be isotropic (q=1).

Finally, Table III presents the amount of plastic volume change at the mid-point of the rod at several times when the "cosine laws" (11) and (38) are used. The Table shows that the amount of volume change when employing the stress "cosine law" (38) is about three times larger than that obtained using (11) with the same value of q. The plastic volume change is therefore a more sensitive indicator of the difference in hardening laws than the stress response for the uniaxial stress case. Which of the two references for anisotropic hardening, i.e. stress or plastic strain rate, is closer to the physical situation is not obvious and will be the subject of further investigations. It is noted that the stress rule (38) leads to simpler numerical work.

Conclusions

Constitutive equations for elastic-viscoplastic anisotropic work-hardening materials proposed by Stouffer and Bodner [3] have been implemented to study the effect of anisotropic hardening and the resulting induced anisotropic plastic flow in several two-dimensional dynamic problems. A basic assumption in the formulation [3] is that anisotropic hardening is controlled by the sign and orientation of the rate of plastic deformation. An alternative formulation could be adopted by taking a "cosine law" based on the current direct stress. These two law are investigated in a uniaxial dynamic problem. Further studies on the applicability and implications of these hardening laws are under investigation.

TABLE I

time $c_o t/H$	$E(0,0,t) \times 10^2$
0.5	0.07
1.0	0.11
1.5	0.13
2.0	0.15
2.5	0.33
3.0	0.54
3.5	0.78
4.0	1.05
4.5	1.31
5.0	1.57

Variation with time of the amount of volume change due to the plastic de-deformation at the point $x_1=x_2=0$ directly under the indenter.

TABLE II

time $c_o t/H$	$E(0,0,t) \times 10^2$	
	rigidly clamped rear surface	traction-free rear surface
0.5	0	0
1.0	-0.21	-0.21
1.5	-0.57	-0.56
2.0	-0.91	-0.58
2.5	-1.14	-0.44
3.0	-1.27	-0.66
3.5	-1.33	-0.80
4.0	-1.40	-0.89
4.5	-1.48	-1.01
5.0	-1.59	-1.19

Variation with time of the amount of volume change due to plastic deformation at the point $x_1=x_2=0$ for a slab loaded at $x_2=0$ when the other surface is rigidly clamped (18) and traction-free (17).

TABLE III

time c_0t/H	amount of volume change due to plastic deformation	
	"strain rate" cosine law (11)	"stress" cosine law (38)
0.5	0	0
1.0	-0.13×10^{-5}	-0.34×10^{-5}
1.5	-0.26×10^{-3}	-0.69×10^{-3}
2.0	-0.40×10^{-3}	-0.11×10^{-2}
2.5	-0.81×10^{-3}	-0.22×10^{-2}
3.0	-0.54×10^{-3}	-0.18×10^{-2}
3.5	-0.53×10^{-3}	-0.18×10^{-2}
4.0	-0.44×10^{-3}	-0.16×10^{-2}
4.5	-0.35×10^{-3}	-0.14×10^{-2}
5.0	-0.35×10^{-3}	-0.14×10^{-2}

Variation with time of the amount of volume change due to plastic deformation at the mid-point of the rod based on the "strain rate" cosine law (11) and the "stress" cosine law (38) for anisotropic hardening.

REFERENCES

1. S.R. Bodner and Y. Partom, "Constitutive Equations for Elastic-Viscoplastic Strain-Hardening Materials," J. Appl. Mech. 42, 385 (1975).

2. J. Aboudi, "The Dynamic Indentation of an Elastic-Viscoplastic Work-Hardening Slab by a Rigid Punch," Int. J. Engng. Sci. (in press).

3. D.C. Stouffer and S.R. Bodner, "A Constitutive Model for the Deformation Induced Anisotropic Plastic Flow of Metals," Int. J. Engng. Sci. 17, 737 (1979).

4. J. Aboudi, "Numerical Solution of Dynamic Stresses Induced by Moving Cracks," Comp. Meth. Appl. Mech. Engng. 9, 301 (1976).

5. J. Aboudi, "The Dynamic Indentation of an Elastic Half-Space by a Rigid Punch," Int. J. Solids Structures 13, 995 (1977).

6. S.R. Bodner, I. Partom and Y. Partom, "Uniaxial Cyclic Loading of Elastic-Viscoplastic Materials," J. Appl. Mech., Trans. ASME, 46 (1979).

7. M.J. Michno and W.N. Findley, "An Historical Perspective of Yield Surface Investigations for Metals," Int. J. Non-Linear Mech. 11, 59 (1976).

FIGURE CAPTIONS

Figure 1: Uniform frictionless indentation of an elastic-viscoplastic anisotropic work-hardening slab (———) and isotropic work-hardening slab (----), by a long rigid circular cylinder with a speed $V/c_o = 0.05$. The plots show the normal and tangential stresses, vertical displacements and plastic work versus the distance along the surface $x_2=0$, and also the plastic work along the plane of symmetry $x_1=0$ within the slab, at times $c_o\ t/H = 2.5$ (top) and $c_o\ t/H = 5$ (bottom).

Figure 2: Time-dependent normal loading of an elastic-viscoplastic anisotropic work-hardening slab (———) and isotropic work-hardening slab (---) whose rear surfaces are rigidly clamped. The plots show the stresses and plastic work versus the distance along $x_2 = H/2$, and also the plastic work along the plane of symmetry $x_1=0$ within the slab, at times $c_o\ t/H = 2.5$ (top) and $c_o\ t/H = 5$ (bottom). The loading function is given by (33).

Figure 3: Same as Figure 2 but for a slab whose rear surface is traction-free.

Figure 4: Axial stress and plastic work versus time at the mid-point of a rod made of elastic-viscoplastic anisotropic work-hardening material whose anisotropic hardening is governed by the "cosine laws" on $\dot{\varepsilon}^p$ (11) (.....), and on σ (38) (----), and for an isotropic work-hardening material (———). The loading function is given by (36).

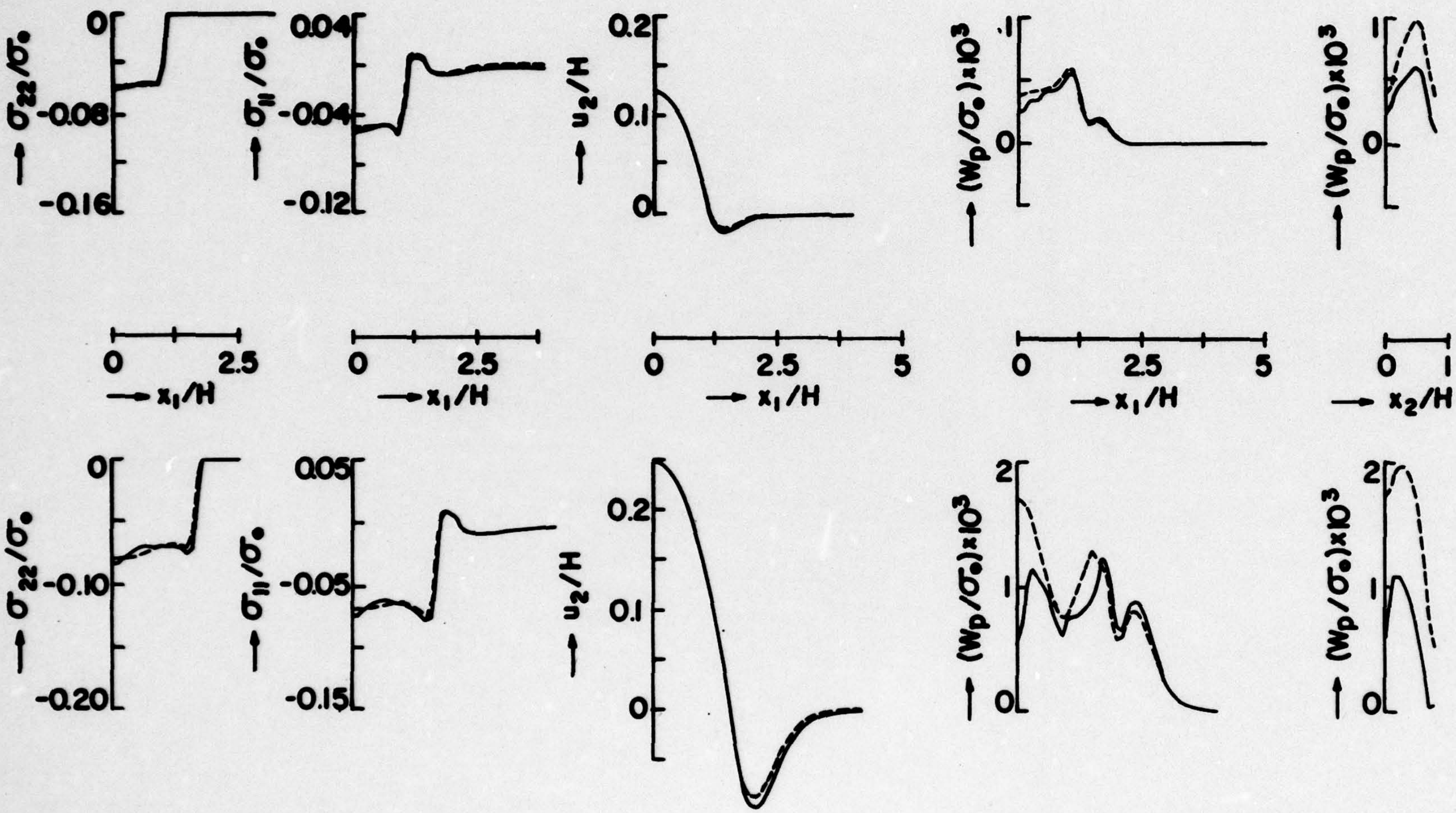

σ_{22}/σ_0
0
-0.08
-0.16
σ_{11}/σ_0
0.04
-0.04
-0.12
u_2/H
0.2
0.1
0
$(W_p/\sigma_0)\times10^3$
1
0
x_1/H
0
2.5
5
x_2/H
1
σ_{22}/σ_0
-0.10
-0.20
σ_{11}/σ_0
0.05
-0.05
-0.15
2

FIG. 1

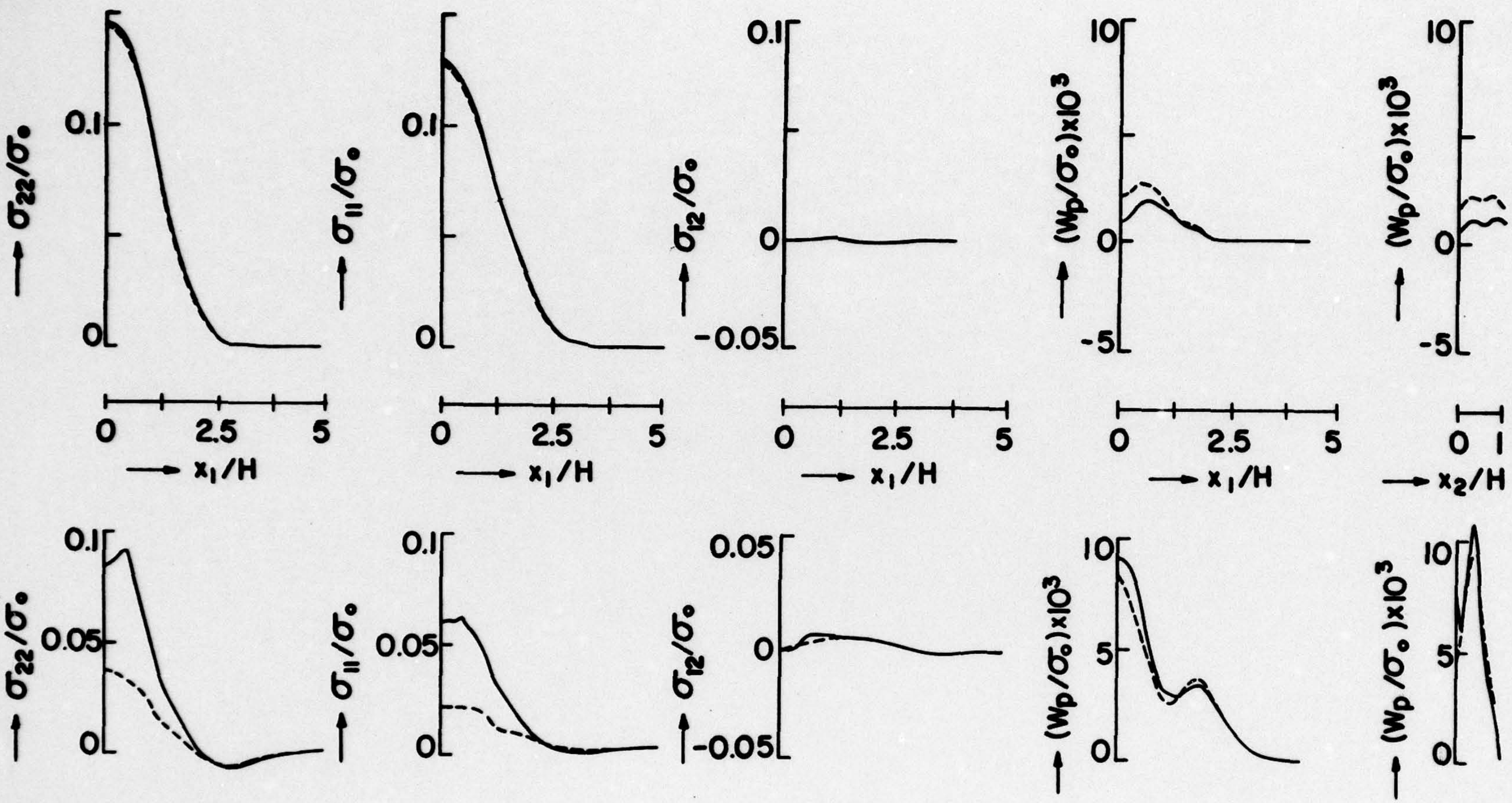
σ_{22}/σ_o
σ_{11}/σ_o
σ_{12}/σ_o
$(W_p/\sigma_o)\times10^3$
x_1/H
x_2/H
0.1
0.05
0
-0.05
10
5
-5
2.5

FIG. 2

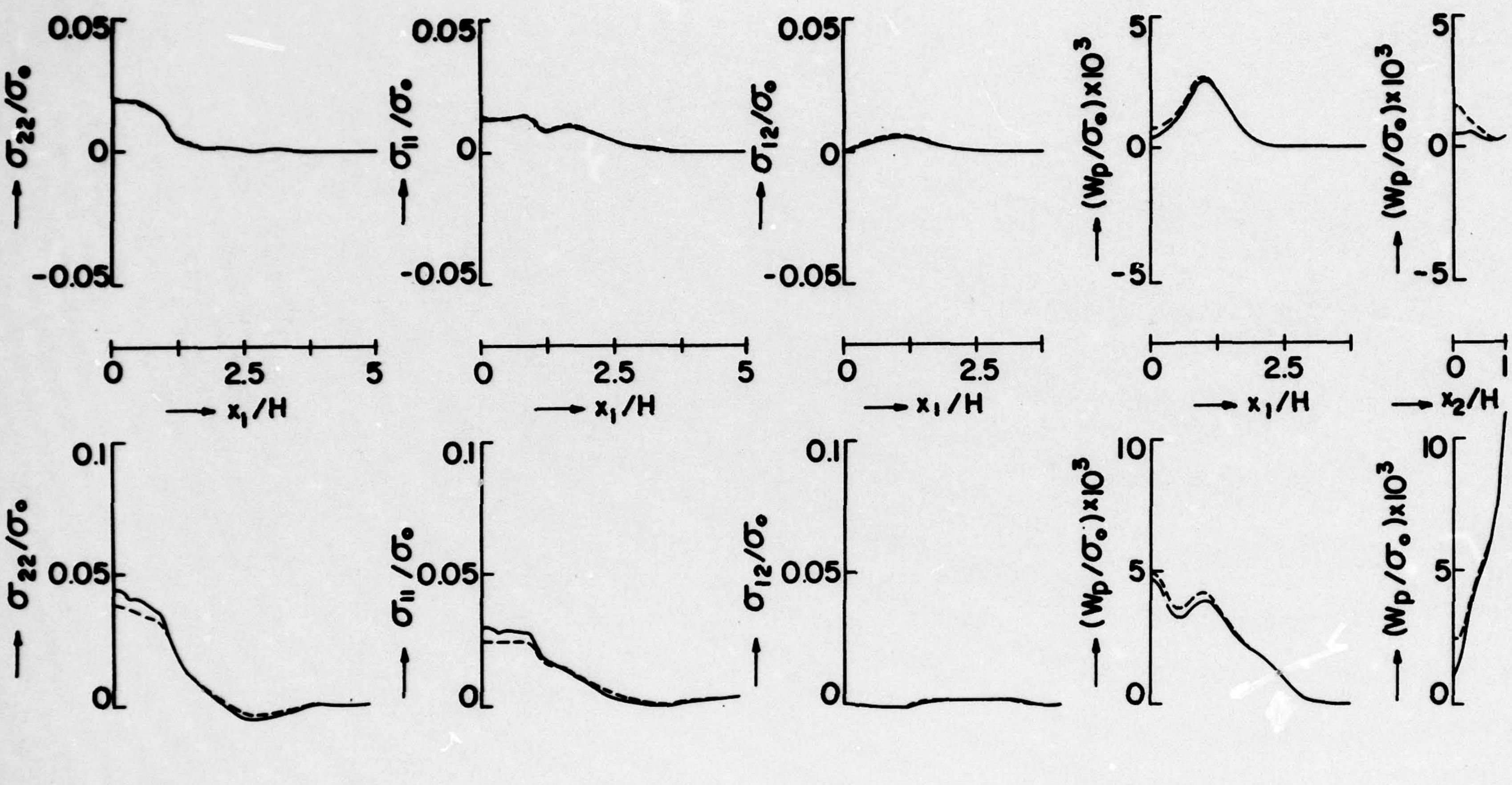

σ_{22}/σ_o
σ_{11}/σ_o
σ_{12}/σ_o
$(W_p/\sigma_o)\times 10^3$
x_1/H
x_2/H
0.05
0
-0.05
0.1
5
-5
10
2.5
1

FIG. 3

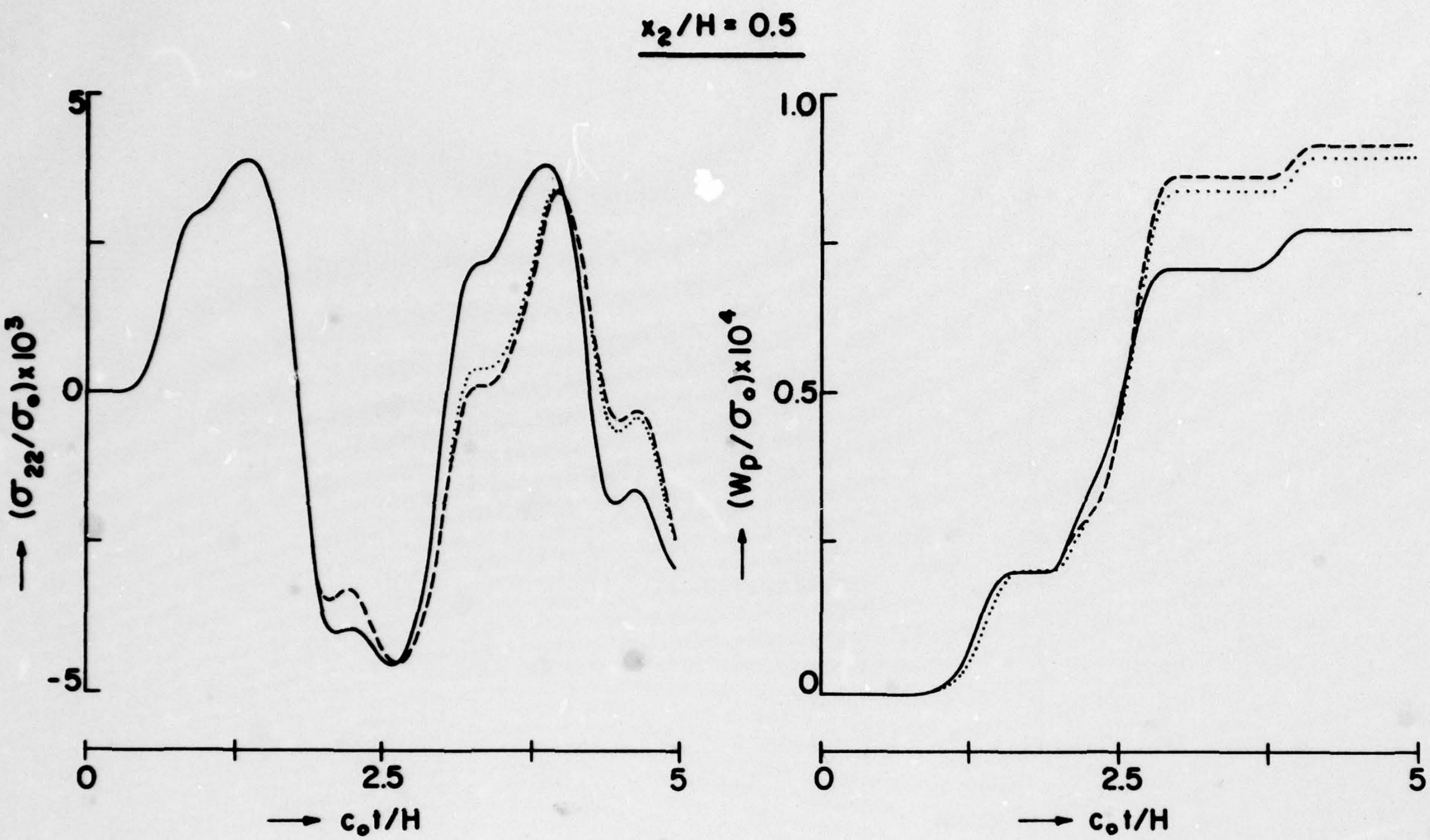

$x_2/H = 0.5$
$\rightarrow (\sigma_{22}/\sigma_o) \times 10^3$
5
0
-5
0
2.5
5
$\rightarrow c_o t/H$
$\rightarrow (W_p/\sigma_o) \times 10^4$
1.0
0.5
0
0
2.5
5
$\rightarrow c_o t/H$

FIG. 4

REPORT DOCUMENTATION PAGE

READ INSTRUCTIONS BEFORE COMPLETING FORM

1. REPORT NUMBER: AFOSR-TR- 79-0964	2. GOVT ACCESSION NO.
3. RECIPIENT'S CATALOG NUMBER	
4. TITLE (and Subtitle): DYNAMIC RESPONSE OF A SLAB OF ELASTIC-VISCOPLASTIC MATERIAL THAT EXHIBITS INDUCED PLASTIC ANISOTROPY	5. TYPE OF REPORT & PERIOD COVERED: INTERIM
	6. PERFORMING ORG. REPORT NUMBER: MML Report No 67
7. AUTHOR(s): J ABOUDI S R BODNER	8. CONTRACT OR GRANT NUMBER(s): F49620-79-C-0196
9. PERFORMING ORGANIZATION NAME AND ADDRESS: TECHNION - ISRAEL INSTITUTE OF TECHNOLOGY MATERIAL MECHANICS LABORATORY HAIFA 32000, ISRAEL	10. PROGRAM ELEMENT, PROJECT, TASK AREA & WORK UNIT NUMBERS: 2307B1 61102F
11. CONTROLLING OFFICE NAME AND ADDRESS: AIR FORCE OFFICE OF SCIENTIFIC RESEARCH/NA BLDG 410 BOLLING AIR FORCE BASE, D C 20332	12. REPORT DATE: Aug 79
	13. NUMBER OF PAGES: 37
14. MONITORING AGENCY NAME & ADDRESS(if different from Controlling Office)	15. SECURITY CLASS. (of this report): UNCLASSIFIED
	15a. DECLASSIFICATION/DOWNGRADING SCHEDULE

16. DISTRIBUTION STATEMENT (of this Report)

Approved for public release; distribution unlimited.

17. DISTRIBUTION STATEMENT (of the abstract entered in Block 20, if different from Report)

18. SUPPLEMENTARY NOTES

19. KEY WORDS (Continue on reverse side if necessary and identify by block number)

CONSTITUTIVE EQUATIONS
DYNAMIC LOADING
VISCOPLASTICITY
ANISOTROPY
WORK HARDENING
INDENTATION

20. ABSTRACT (Continue on reverse side if necessary and identify by block number)

Various two-dimensional problems of the dynamic loading of a slab are solved for a material characterization that is elastic-viscoplastic and exhibits anisotropic work-hardening. The governing constitutive equations are based on a unified formulation which requires neither a yield criterion nor loading or unloading conditions. They include multi-dimensional anisotropic effects induced by the plastic deformation history. The theory also considers plastic compressibility which depends on the extent of anisotropy. A numerical procedure for solving equations is developed which incorporates the history dependent anisotropic

hardening effects. Cases considered are the dynamic penetration of a slab by a rigid cylindrical indenter, and a distributed force rapidly applied over part of the slab surface. Both conditions of fixed and free rear surfaces of the slab are examined. A uniaxial problem is also considered in which different bases for the anisotropic hardening law are examined.